A Software Tool for Retrieving Land Surface Temperature from ASTER Imagery

Hakan OĞUZ[a]

[a]*Kahramanmaraş Sütçü İmam University, Faculty of Forestry, Department of Landscape Architecture, 46100, Kahramanmaraş, TURKEY*

ABSTRACT

Remote sensing is a powerful and well-known tool in the collection, analysis, and modeling of environmental data, however, not much attention has been given to the use of thermal infrared (TIR) remote sensing. Land surface temperature (LST) is a key parameter for many environmental studies such as global environmental change, climate models, and human-environment interactions. In this study, a software tool which retrieves LST from Advanced Spaceborne Thermal Emission and reflection Radiometer (ASTER) imagery has been developed in Visual Basic .NET. The tool consists of five main modules: 1- Converting DN to Radiances, 2- Calculating surface reflectances, 3- Calculating NDVI, 4- Calculating emissivity and 5- Calculating surface temperature. In this tool, Jimenez Munoz and Sobrino's Single Channel ($SC^{JM\&S}$) Algorithm for ASTER was employed. With this tool, user can be able to calculate LST using (1) atmospheric parameters such as atmospheric transmissivity, upwelling and downwelling atmospheric radiances, (2) atmospheric water-vapor content. Hopefully, this program will be a useful tool for scientists/persons who are interested in studying thermal environments.

Keywords: Urban climate; Urban heat island; Thermal infrared remote sensing; Atmospheric parameters; Water-vapor content; Visual Basic.NET

ASTER Uydu Görüntüsünden Yer Yüzey Sıcaklığını Hesaplayan Bir Yazılım Aracı Geliştirilmesi

ÖZET

Çevresel verinin toplanması, analizi ve modellemesinde uzaktan algılama çok önemli ve iyi bilinen bir araç olmasına rağmen, termal kızılötesi (TIR) uzaktan algılamasına gereken önem verilmemiştir. Küresel çevre değişimi, iklim modelleri ve insan-çevre etkileşimleri gibi birçok çevresel çalışmalar için yer yüzey sıcaklığı (LST) önemli bir parametredir. Bu çalışmada, Visual Basic NET programlama dili kullanılarak ASTER uydu görüntüsünden yer yüzey sıcaklığını

hesaplayan bir yazılım aracı geliştirilmiştir. Bu araç beş modülden oluşmaktadır: 1- Dijital Sayıları (DN) Radyansa dönüştürme, 2- Yüzey yansıma değerinin hesaplanması, 3- NDVI'ın hesaplanması, 4- Yayınırlığın hesaplanması ve 5- Sıcaklığın hesaplanması. Bu yazılım aracında Jimenez Munoz ve Sobrino'nun ASTER uydu görüntüsünden yer yüzey sıcaklığının hesaplanması için geliştirdiği Tek Kanal (Single Channel) Algoritması kullanılmıştır. Bu programın termal çevre üzerine çalışan bilim insanları veya konuyla ilgilenen kişiler için faydalı olabileceği ümit edilmektedir.

1. Introduction

Urban heat island effect, global warming, enhanced green-house effects and other environmental problems have become very important subjects to overcome in the last decades. Land surface temperature is an important parameter for many environmental models (Xiao et al 2007). LST retrieval using remotely sensed data is the most popular subjects in environmental studies during the last couple of decades (Genc et al 2010).

The ASTER on the NASA's Terra platform is the highest spatial resolution with 90 m multispectral TIR sensor currently available on a polar-orbiting spacecraft. The accuracies for temperature and emissivity separation (TES) algorithm were found to be within the specifications of ±0.015 for emissivity and ±1.5 K for LST. However, some inaccuracies have been found over agricultural areas. These problems were pointed out in Gillespie et al (1998) and have been explicitly analyzed and those problems were partially avoided over agricultural areas by Jimenez-Munoz et al (2006); Gustafson et al (2006) and Sobrino et al (2007). Another method was developed by Jimenez-Munoz & Sobrino (2007) using split-window (SW) algorithms to retrieve LST from ASTER imagery, where input emissivities can be calculated from the normalized difference vegetation index (NDVI) (Jimenez-Munoz et al 2006). Results retrieved from this methods howed similar errors to those specified for TES products.

Currently, there are two programs developed for LST retrieval from Landsat imagery (Zhang et al 2006; Oguz 2013), however, no software tools were developed for ASTER imagery yet. Therefore, in this particular study, a program was developed in order to retrieve LST from ASTER imagery. In this tool, a single-channel (SC) algorithm developed by Jimenez-Munoz & Sobrino (2010) was employed, which was oriented for people who:

- are interested in LST retrieval but not familiar with TES products
- cannot get TES products, or
- have found unsatisfactory results by using TES products, so prefer another method different than the SW algorithm mentioned earlier. This algorithm is easy to implement and also based on the procedure formulated by Jimenez-Munoz & Sobrino (2003). It has been designed for ASTER satellite imagery based on the algorithm developed for Landsat TIR imagery (Jimenez-Munoz et al 2009). The algorithm is hereinafter denoted as SC[JM&S].

2. Material and Methods

2.1. ASTER imagery

The ASTER was launched on NASA's Terra spacecraft in 1999, and each scene contains 14 bands from visible to thermal infrared region with coverage of 60 x 60 km area. ASTER contains three different band groups (Table 1); in the first group, there are four bands within the Visible and Near-infrared (VNIR) region with a spatial resolution of 15 m; in the second group, there are six bands in the Shortwave Infrared (SWIR) region with a spatial resolution of 30 m and in the third and final group, there are five bands within TIR region with a spatial resolution of 90 m (Abrams et al 2008).

Table 1- Characteristics of the ASTER sensor systems (Abrams et al 2008)

Çizelge 1- ASTER sensör sistemlerinin özellikleri (Abrams et al 2008)

Subsystem	Band number	Spectral range (μm)	Spatial resolution (m)	Quantization levels
VNIR	1	0.52 – 0.60	15	8 bits
	2	0.63 – 0.69		
	3N	0.78 – 0.86		
	3B	0.78 – 0.86		
SWIR	4	1.60 – 1.70	30	8 bits
	5	2.145 – 2.185		
	6	2.185 – 2.225		
	7	2.235 – 2.285		
	8	2.295 – 2.365		
	9	2.360 – 2.430		
TIR	10	8.125 – 8.475	90	12 bits
	11	8.475 – 8.825		
	12	8.925 – 9.275		
	13	10.25 – 10.95		
	14	10.95 – 11.65		

The single-channel (SC$^{JM\&S}$) algorithm

The SC$^{JM\&S}$ algorithm calculates LST (T_S) using the Equation 1.

$$T_s = \gamma[(1/\varepsilon)(\psi_1 L_{sen} + \psi_2) + \psi_3] + \delta \qquad (1)$$

Where; ε is the surface emissivity; is the at-sensor registered radiances; γ and δ are two parameters dependent on the Planck's equation, and ψ_1, ψ_2 and ψ_3 are referred to as atmospheric parameters (AP) and given in Equation 2.

$$\psi_1 = (1/\tau), \psi_2 = -L^{\downarrow} - (L^{\uparrow}/\tau), \quad \psi_3 = L^{\downarrow} \quad (2)$$

Where; is the atmospheric transmissivity; $L^{\uparrow}$ is the upwelling atmospheric radiance, and $L^{\downarrow}$ is the downwelling atmospheric radiance. It is also essential to convert at-sensor registered radiances (L_{sen}) into at-sensor brightness temperatures (T_{sen}) especially when working with thermal bands. T_{sen} is computed using inversion of the Planck's law (Jimenez-Munoz & Sobrino 2010) and presented in Equation 3.

$$T_{sen} = K_2 / \ln\left(\frac{K_1}{L_{sen}} + 1\right) \qquad (3)$$

Where; K_1 and K_2 are the radiation constants which are given in Table 2.

Table 2- Radiation constants used in Equation 3

Çizelge 2- Eşitlik 3'te kullanılan radyasyon sabit değerleri

ASTER Band	K_1 (W m^2 sr^{-1} μm^{-1})	K_2 (K)
10	3047.47	1736.18
11	2480.93	1666.21
12	1930.80	1584.72
13	865.65	1349.82
14	649.60	1274.49

Parameters γ and δ used in Equation 1 can be calculated by Equation 4.

$$\gamma \approx (T_{sen}^2/K_2 L_{sen}), \ \delta \approx T_{sen} - (T_{sen}^2/K_2) \quad (4)$$

Where; T_{sen} is computed using Equation (3) and K_2 can be retrieved from Table 2.

Even though the APs can be computed in a number of different ways as explained by Jimenez-Munoz & Sobrino (2010), the SC$^{JM\&S}$ method was selected and used in this particular study due to the fact that the model requires minimal and more accessible input data. The atmospheric parameters; τ, $L^{\uparrow}$ and $L^{\downarrow}$ can be computed using the local atmospheric sounding and MODTRAN.

Atmospheric parameters can also be obtained from second-order polynomial fits versus the atmospheric water-vapor content (Jimenez-Munoz & Sobrino 2003; Jimenez-Munoz & Sobrino 2007; Jimenez-Munoz & Sobrino 2010) as shown in Equation 5.

$$\begin{bmatrix} \psi_1 \\ \psi_2 \\ \psi_3 \end{bmatrix} = \begin{bmatrix} c_{11} & c_{12} & c_{13} \\ c_{21} & c_{22} & c_{23} \\ c_{31} & c_{32} & c_{33} \end{bmatrix} \begin{bmatrix} \omega^2 \\ \omega \\ 1 \end{bmatrix} \quad (5)$$

Where; coefficients c_{ij} are obtained from simulated data constructed from atmospheric profiles as described in Jimenez-Munoz & Sobrino (2010) (Table 3).

Table 3- Coefficients for the atmospheric functions following matrix notation in Equation 5 (Jimenez-Munoz & Sobrino 2010)

Çizelge 3- Eşitlik 5'te kullanılan katsayı değerleri (Jimenez-Munoz & Sobrino 2010)

Database	Band	Cij	i=1	i=2	i=3
		j=1	0.06524	-0.05878	1.06576
STD66	13	j=2	-0.55835	-0.75881	0.00327
		j=3	-0.00284	1.35633	-0.43020
		j=1	0.05327	-0.03937	1.05742
TIGR61	13	j=2	-0.48444	-0.74611	-0.03015
		j=3	0.00764	1.24532	-0.39461
		j=1	0.10062	-0.13563	1.10559
STD66	14	j=2	-0.79740	-0.39414	-0.17664
		j=3	-0.03091	1.60094	-0.56515
		j=1	0.07965	-0.09580	1.08983
TIGR61	14	j=2	-0.66528	-0.48582	-0.17029
		j=3	-0.01578	1.46358	-0.52486

2.2. NDVI retrieval

Normalized difference vegetation index (NDVI) for an ASTER imagery is calculated using bands 2 (RED) and 3N (NIR). Atmospheric correction procedure must be done before NDVI calculation due to the fact that atmospheric effects contaminate NDVI signals (Song et al 2001). Therefore, ASTER imagery is atmospherically corrected using the image-based atmospheric correction method developed by Chavez (1996) before calculating NDVI. This method is applied to the raw DN values of ASTER bands 2 and 3N. Atmospherically and radiometrically corrected surface reflectance of bands 2 and 3 are derived and used thereafter for the calculation of NDVI. NDVI is calculated from the atmospherically corrected reflectivity of ASTER bands as shown in Equation 6.

$$NDVI = (\rho_{band3} - \rho_{band2}/\rho_{band3} + \rho_{band2}) \quad (6)$$

Where; ρ_{band3} is the spectral reflectance of near-infrared band and ρ_{band2} represents the spectral reflectance of red band.

2.3. Emissivity retrieval using NDVI values

Jimenez-Munoz et al (2006) states emissivity as a proportionality factor, that scales black body radiance (Planck's law) to estimate emitted radiance. Therefore, emissivity must be obtained beforehand to retrieve LST accurately. Several approaches have been proposed over the years to retrieve land surface emissivity from NDVI (Van de Griend & Owe 1993; Valor & Caselles 1996; Sobrino & Raissouni 2000; Jimenez-Munoz et al 2006). In this study, Jimenez-Munoz et al (2006) approach has been adopted to retrieve land surface emissivity using NDVI values since this method has been tested against in situ measurements by the authors. The results indicated that this method gave root mean square errors (RMSE)<0.005 over vegetated areas. This approach is based on the following simplified Equation 7.

$$\varepsilon_i = \varepsilon_{vi}P_v + \varepsilon_{si}(1 - P_v) \quad (7)$$

Where; ε_{vi} and ε_{si} represent vegetation and bare soil band emissivity values respectively, and P_v is the vegetation proportion. According to Carlson & Ripley (1997), vegetation proportion (P_v) is computed from NDVI values as shown in Equation 8.

$$P_v = \left[\frac{NDVI - NDVI_s}{NDVI_v - NDVI_s} \right]^2 \quad (8)$$

Where; $NDVI_v = 0.5$; $NDVI_s = 0.2$. According to Jimenez-Munoz et al (2006), Equation 8 provides reasonable results with an accuracy of around 15%, which is a value acceptable to retrieve surface emissivities from Equation (7). NDVI values are obtained from the atmospherically corrected reflectivity of ASTER bands 2 (RED) and 3 (NIR). For those pixels with NDVI<$NDVI_s$ P_v is set to zero, whereas for those pixels with NDVI>$NDVI_v$ it is set to 1. Finally surface emissivities for ASTER thermal bands can be computed as shown in Equation 9a-9e (Carlson & Ripley 1997; Jimenez-Munoz et al 2006):

$$\varepsilon_{10} = 0.946 + 0.044\, P_v \qquad (9a)$$

$$\varepsilon_{11} = 0.949 + 0.041\, P_v \qquad (9b)$$

$$\varepsilon_{12} = 0.941 + 0.049\, P_v \qquad (9c)$$

$$\varepsilon_{13} = 0.968 + 0.022\, P_v \qquad (9d)$$

$$\varepsilon_{14} = 0.970 + 0.020\, P_v \qquad (9e)$$

According to Jimenez-Munoz & Sobrino (2010) bands 13 and 14 of ASTER are the best for LST calculation with this SC algorithm. Therefore, band 14 has been employed in the program for LST retrieval.

3. Results and Discussion

3.1. The software tool

This tool was written in Visual Basic .NET and can be run on Microsoft Windows operating systems. There are five menus in the tool: 1- Radiance, 2- Reflectance, 3- NDVI, 4- Emissivity, and 5- Temperature. The flowchart of the program can be seen in Figure 1 below. At sensor Radiances for ASTER bands are computed from Equation 10 (Milder 2008; Ghulam 2009).

$$L_{sen} = (DN - 1) * UCC \qquad (10)$$

Where; L_{sen} is at sensor radiance, DN represents digital number, and UCC is unit conversion coefficient. UCC values can be obtained from Table 4 below according to band's gain setting. Furthermore, Figures 2 and 3 illustrate the radiance calculation interface of the software tool.
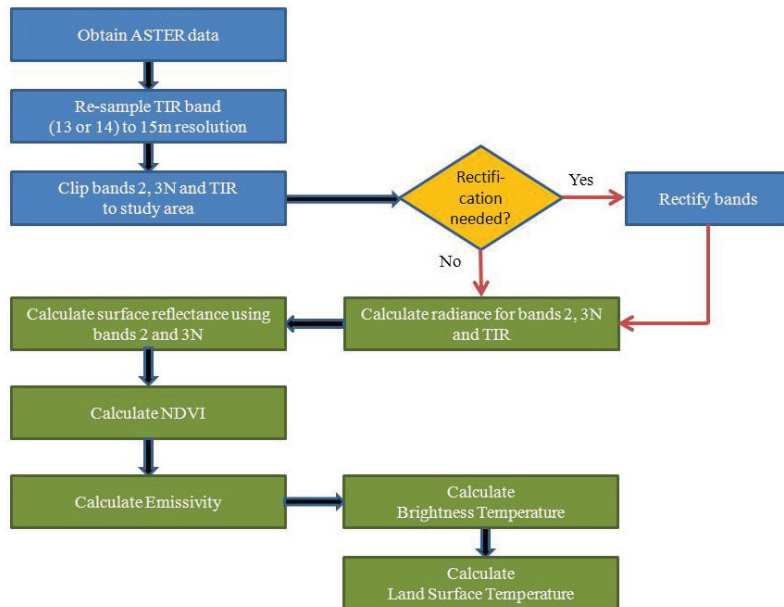
Figure 1- Flowchart for the program

Şekil 1- Programın akış şeması

Table 4- ASTER unit conversion coefficients (UCC) (Ghulam 2009)

Çizelge 4- ASTER birim dönüştürme katsayıları (BDK) (Ghulam 2009)

Band	ASTER UCC ($W\ m^{-2}*sr*um$)/DN			
	High gain	Normal	Low gain 1	Low gain 2
1	0.676	1.688	2.25	
2	0.708	1.415	1.89	NA
3N	0.423	0.862	1.15	
3B	0.423	0.862	1.15	
4	0.1087	0.2174	0.2900	0.2900
5	0.0348	0.0696	0.0925	0.4090
6	0.0313	0.0625	0.0830	0.390
7	0.0299	0.0597	0.0795	0.332
8	0.0209	0.0417	0.0556	0.245
9	0. 0159	0.0318	0.0424	0.265
10		0.006822		
11		0.006780		
12	NA	0.006590	NA	NA
13		0.005693		
14		0.005225		
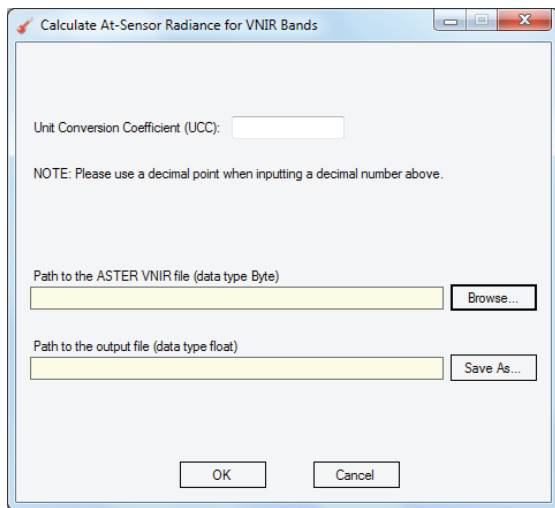
Figure 2- Radiance calculation interface for ASTER VNIR bands

Şekil 2- ASTER görünür yakın kızılötesi bantları için radyans hesaplama arayüzü
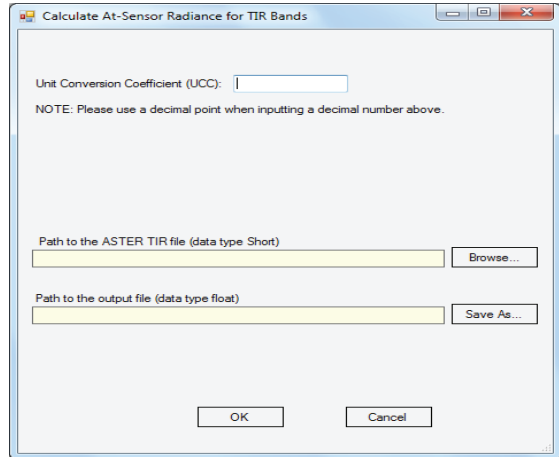
Figure 3- Radiance calculation interface for ASTER TIR bands

Şekil 3- ASTER termal bantları için radyans hesaplama arayüzü

After calculating at sensor radiances, planetary reflectances for ASTER bands (2 and 3N only) are computed using the Equation 11 (Ghulam 2009):

$$\rho_{TOA} = (\pi * L_{sen} * d^2 / E_{SUN} * \cos(\theta)) \quad (11)$$

Where; is unitless planetary reflectance; L_{sen} is at sensor radiance; d is Earth-Sun distance in astronomical units (populated from Table 5); E_{SUN} is mean solar exoatmospheric irradiances (Table 6), and represents solar zenith angle in degrees.

Figure 4 shows the planetary reflectance calculation step of the program. This step requires four parameters: Julian Day, Mean Solar Exoatmospheric Irradiances, Solar Elevation Angle in Degrees, and Dark Object Value. Julian Day represents the day numbers based on acquisition date of the ASTER imagery. Mean Solar Exoatmospheric Irradiances can be obtained from Table 6 above and Solar Elevation angle is given in the header file. Dark Object value represents the area of zero reflectance below the pixel with the lowest reflectance values in the image. NDVI values can be computed easily after planetary reflectance values are calculated for ASTER bands 2 and 3 as illustrated in Figure 5 below. Afterwards, this NDVI file is used as an input to calculate emissivity values shown in Figure 6. The brightness temperature calculation step requires K_1 and K_2 radiation constants, which can be

Table 5- Earth-sun distance (in astronomical units) (Ghulam 2009)

Çizelge 5- Dünya-Güneş mesafesi (astronomik birim) (Ghulam 2009)

					Earth-Sun distance in astronomical distance				
DOY	Distance	DOY	Distance	DOY	Distance	DOY	Distance	DOY	Distance
1	0.98331	74	0.99446	152	1.01403	227	1.01281	305	0.99253
15	0.98365	91	0.99926	166	1.01577	242	1.00969	319	0.98916
32	0.98536	106	1.00353	182	1.01667	258	1.00566	335	0.98608
46	0.98774	121	1.00756	196	1.01646	274	1.00119	349	0.98426
60	0.99084	135	1.01087	213	1.01497	288	0.99718	365	0.98333

Table 6- ASTER mean solar exoatmospheric irradiances (Ghulam 2009)

Çizelge 6- ASTER ortalama güneş exoatmospheric irradyans değerleri (Ghulam 2009)

Band	Smith: E_{SUN}	Thome et al (A): E_{SUN}	Thome et al (B): E_{SUN}
1	1845.99	1847	1848
2	1555.74	1553	1549
3N	1119.47	1118	1114
3B	NA	NA	NA
4	231.25	232.5	225.4
5	79.81	80.32	86.63
6	74.99	74.92	81.85
7	68.66	69.20	74.85
8	59.74	59.82	66.49
9	56.92	57.32	59.85

obtained from Table 2, and the radiance file for the thermal band as shown in Figure 7 below.
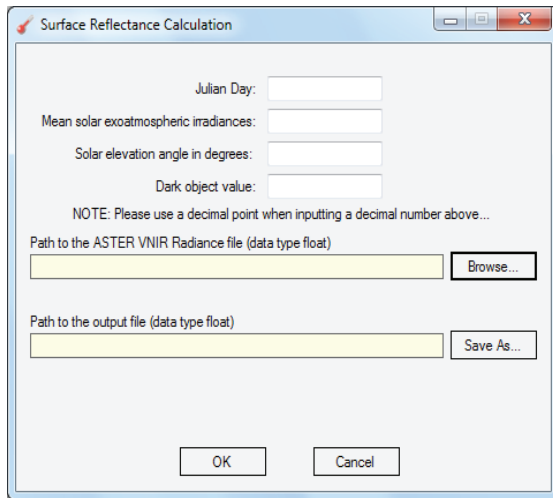
Figure 4- Reflectance calculation interface

Şekil 4- Yansıma hesaplama arayüzü
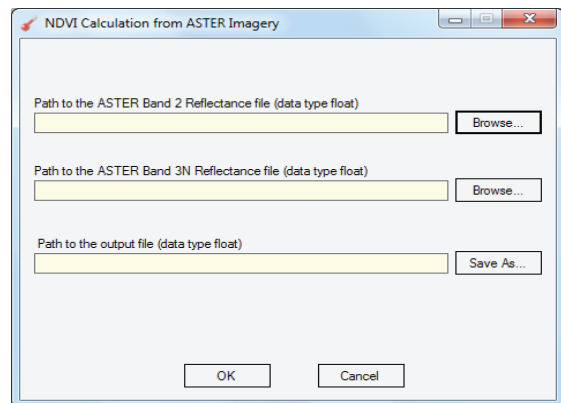
Figure 5- NDVI calculation interface

Şekil 5- NDVI hesaplama arayüzü
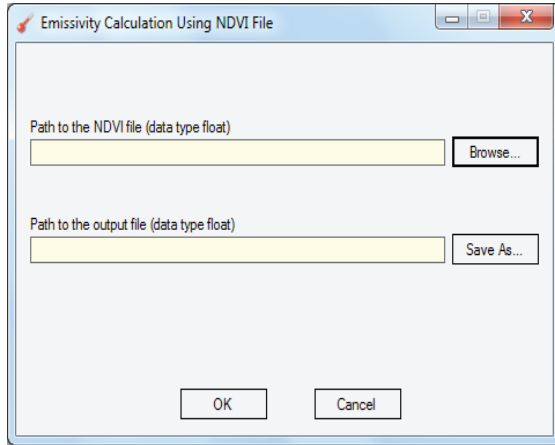
Figure 6- Emissivity calculation interface

Şekil 6- Yayınırlık hesaplama arayüzü
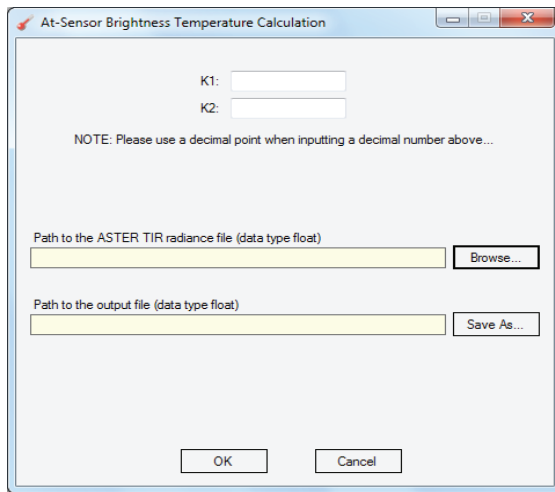
Figure 7- Brightness temperature calculation interface

Şekil 7- Parlaklık sıcaklığı hesaplama arayüzü

Finally, user can calculate the LST using either atmospheric parameters such as atmospheric transmissivity, upwelling and downwelling atmospheric radiances as seen in Figure 8, which can be obtained from MODTRAN4 (Berk et al 2003); or atmospheric water-vapor content as illustrated in Figure 9. This tool uses STD66 database values for ASTER band 14 from Table 3 during the calculation of LST using atmospheric water-vapor content.

ASTER bands and processed files such as radiance, NDVI, reflectance, emissivity etc. can be opened by using image processing programs such as ENVI after inputting image samples and lines correctly.
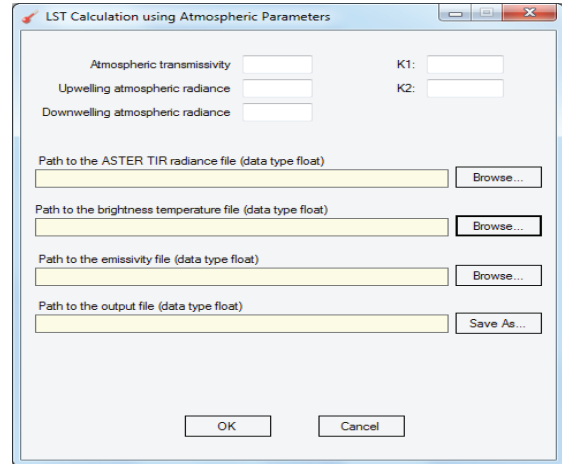
Figure 8- LST retrieval interface using atmospheric parameters

Şekil 8- Atmosferik parametreler kullanılarak yer yüzey sıcaklığının elde edildiği arayüz
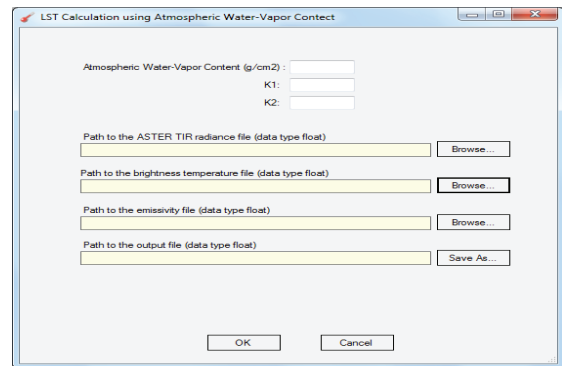
Figure 9- LST retrieval interface using atmospheric water-vapor content

Şekil 9- Atmosferik su buharı içeriği kullanılarak yer yüzey sıcaklığının elde edildiği arayüz

3.2. Application of the program

In this part of the study, Baltimore, the largest city of Maryland and the 24th most populous city in

the United States, is provided for demonstration purposes (Figure 10). An ASTER scene (Level 1B, path/row: 15/33), acquired on August 24 2003, was downloaded from GLCF (Global Land Cover Facility) website (http://glcf.umiacs.umd. edu/). TIR bands originally have 90 m resolution, so they were resampled using the nearest neighbor algorithm with spatial resolution of 15 m to make

them match to VNIR bands. The sample files used for demonstration are listed in Table 7. The ASTER imagery with 15 m spatial resolution and dimension of 5729 x 5124 was used as an example for LST retrieval in this study. The parameters for the ASTER imagery used during LST retrieval in the program are illustrated in Table 8.
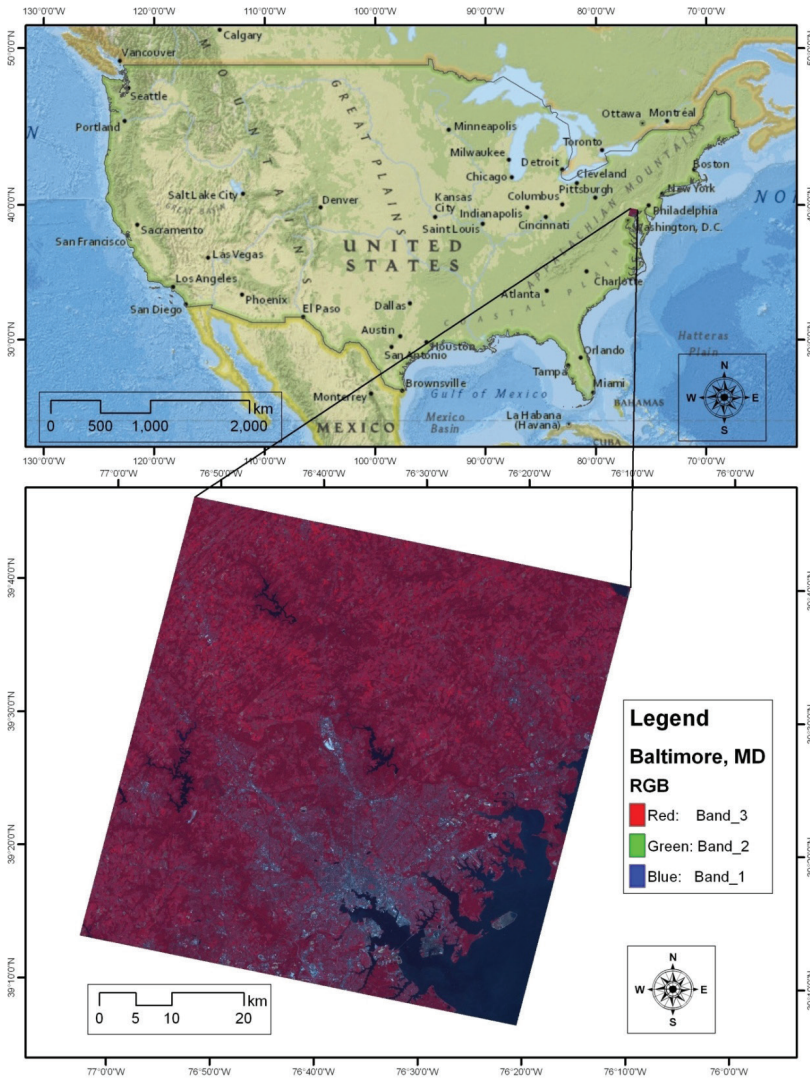
Figure 10- ASTER scene of Baltimore used during the implementation of the software tool

Şekil 10- Programın uygulamasında kullanılan Baltimore ASTER görüntüsü

Table 7- Files used in the program during demonstration

Çizelge 7- Uygulama esnasında programda kullanılan dosyalar

File name	Data type	File dimension	Description
Band2	Byte	5729 x 5124	ASTER band 2
Band2.hdr	Txt	5729 x 5124	Header file of band 2
Band3N	Byte	5729 x 5124	ASTER band 3N
Band3N.hdr	Txt	5729 x 5124	Header file of band 3N
Band14	Short	5729 x 5124	ASTER band 14 (TIR band)
Band14.hdr	Txt	5729 x 5124	Header file of band 14
Band2rad	Float	5729 x 5124	At-sensor radiance file of band 2
Band2rad.hdr	Txt	5729 x 5124	Header file of band 2 radiance file
Band3Nrad	Float	5729 x 5124	At-sensor radiance file of band 3N
Band3Nrad.hdr	Txt	5729 x 5124	Header file of band 3N radiance file
Band14rad	Float	5729 x 5124	At-sensor radiance file of band 14
Band14rad.hdr	Txt	5729 x 5124	Header file of band 14 radiance file
Band2ref	Float	5729 x 5124	Planetary reflectance file of band 2
Band2ref.hdr	Txt	5729 x 5124	Header file of band 2 reflectance file
Band3Nref	Float	5729 x 5124	Planetary reflectance file of band 3N
Band3Nref.hdr	Txt	5729 x 5124	Header file of band 3N reflectance file
Ndvi	Float	5729 x 5124	NDVI file
Ndvi.hdr	Txt	5729 x 5124	Header file of NDVI file
Emissivity	Float	5729 x 5124	Emissivity file
Emissivity.hdr	Txt	5729 x 5124	Header file of emissivity file
BrightTemp	Float	5729 x 5124	Brightness temperature file
BrightTemp.hdr	Txt	5729 x 5124	Header file of brightness temperature file
LST	Float	5729 x 5124	Land surface temperature file
LST.hdr	Txt	5729 x 5124	Header file of land surface temperature file

Table 8- Parameters for sample ASTER data used in the program

Çizelge 8- Programda kullanılan örnek ASTER verisine ait parametreler

Parameter name	Value
UCC (Unit Conversion Coefficient) for Band 2	0.708
UCC (Unit Conversion Coefficient) for Band 3N	0.862
UCC (Unit Conversion Coefficient) for Band 14	0.005225
Julian Day (the day of the year)	236
Mean solar exoatmospheric irradiances for Band 2	1555.74
Mean solar exoatmospheric irradiances for Band 3N	1119.47
Solar elevation angle (in degrees)	57.9062
Dark object value for Band 2	22
Dark object value for Band 3N	18
K_1 for Band 14	649.60
K_2 for Band 14	1274.49
Atmospheric transmission	0.87
Upwelling radiance	1.01
Downwelling radiance	1.69

The final LST distribution map of Baltimore, MD that was calculated using atmospheric parameters was given in Figure 11. As illustrated in Figure 11, the minimum and maximum temperatures of the scene were computed as 278 K (4.85 ºC) and 335 K (61.85 ºC). Maximum temperatures were retrieved within dense urban areas while minimum temperatures were calculated in water and forested areas.
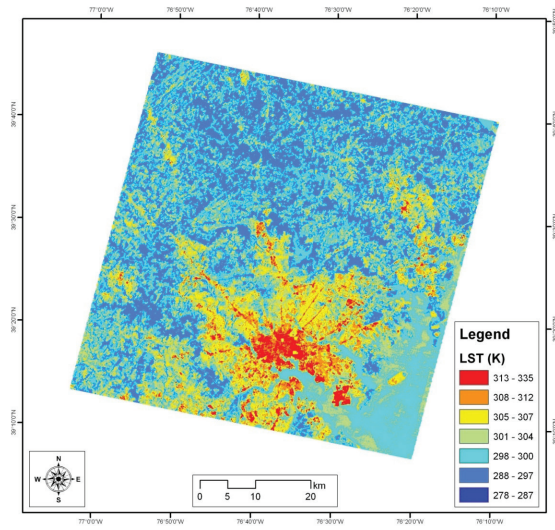
Figure 11- Spatial distribution of the LST in the study area

Şekil 11- Çalışma alanındaki yer yüzey sıcaklığının konumsal dağılımı

4. Conclusions

In this study, a software tool was developed to calculate LST from ASTER imagery using either atmospheric parameters or atmospheric water-vapor content. This software can be an invaluable tool for those who are interested in thermal environment of earth's surface by using ASTER imagery. This tool employs Jimenez-Munoz & Sobrino's Single Channel (SC$^{JM\&S}$) Algorithm for ASTER and detailed information regarding the algorithm can be found in Jimenez-Munoz & Sobrino (2010). The precision of the LST calculated with this software tool depends highly on the algorithms and the parameters used.

There are still some constraints for the software tool. Users must know the input bands' data type as well as their number of lines and rows so that those files can be opened by other image processing software. Input data files must have no offset (head size) as in EXELIS ENVI™ data type. The final LST file calculated by this software can be opened in EXELIS ENVI™ after inputting the header information. Furthermore, some atmospheric parameters are required prior to the calculation such as atmospheric transmissivity, upwelling and downwelling radiances, which are essential to the retrieval of LST. These atmospheric parameters can be obtained from atmospheric soundings and radiative transfer models such as MODTRAN4.

Acknowledgments

References

Abrams M, Hook S & Ramachandran B (2008). ASTER user handbook: Version 2, Jet Propulsion Laboratory, Pasadena, CA, USA

Berk A, Anderson G, Acharya P, Hoke M, Chetwynd J, Bernstein L, Shettle E, Matthew M & Adler-Golden S (2003). MODTRAN4 Version 3 Revision 1 User's Manual, Air Force Res. Lab., Hanscom Air Force Base, Mass

Carlson T N & Ripley D A (1997). On the relation between NDVI, fractional vegetation cover, and leaf area index. *Remote Sensing of Environment* **62**: 241-252

Chavez P S (1996). Image-based atmospheric correction–revisited and improved. *Photogrammetric Engineering & Remote Sensing* **62**(9): 1025-1036

Genc L, Sacan M, Turhan H, Asar B (2010). Arazi örtüsünün Landsat TM uydu görüntüleri yardımıyla belirlenmesi. *Tarım Bilimleri Dergisi – Journal of Agricultural Sciences* **16**: 213-224

Ghulam A (2009). How to calculate reflectance and temperature using ASTER data, Center for Environmental Sciences at Saint Louis University. http://www.pancroma.com/ downloads/ASTER%20 Temperature%20and%20Reflectance.pdf, (Access time: 15 March 2012)

Gillespie A, Rokugawa S, Matsunaga T, Cothern J S, Hook S & Kahle A B (1998). A temperature and emissivity separation algorithm for advanced spaceborne thermal emission and reflection radiometer (ASTER) images. *IEEE Transactions on Geoscience and Remote Sensing* **36**(4): 1113–1126

Gustafson W T, Gillespie A & Yamada G J (2006). Revisions to the ASTER temperature/emissivity separation algorithm. In: *Proceedings of Recent Advancesin Quantitative Remote Sensing*, Valencia, Spain, September 25–29, pp. 770–775

Jimenez-Munoz J C & Sobrino J A (2003). A generalized single-channel method for retrieving land surface temperature from remote sensing data. *Journal of Geophysical Research* **108**(D22): 4688, doi:10.1029/2003JD003480

Jimenez-Munoz J C & Sobrino J A (2007). Feasibility of retrieving land-surface temperature from ASTER TIR bands using two-channel algo-rithms: A case study of agricultural areas. *IEEE Geoscience and Remote Sensing Letters* **4**(1): 60–64

Jimenez-Munoz J C & Sobrino J A (2010). A single-channel algorithm for land surface temperature retrieval from ASTER data. *IEEE Geoscience and Remote Sensing Letters* **7**(1): 176-179

Jimenez-Munoz J C, Sobrino J A, Gillespie A, Sabol D & Gustafson W T (2006). Improved land surface emissivities over agricultural areas using ASTER NDVI. *Remote Sensing of Environment* **103**(4): 474–487

Jimenez-Munoz J C, Cristobal J, Sobrino J A, Soria G, Ninyerola M & Pons X (2009). Revision of the single-channel algorithm for land surface temperature retrieval from Landsat thermal-infrared data. *IEEE Transactions on Geoscience and Remote Sensing* **47**(1): 339–349

Milder J C (2008). ASTER processing method. Department of Natural Resource, Cornell University

Oguz H (2013). LST Calculator: a program retrieving land surface temperature from Landsat TM/ETM+ Imagery. *Environmental Engineering and Management Journal* **12**(3): 549–555

Sobrino J A, Jimenez-Munoz J C, Balick L, Gillespie A, Sabol D & Gustafson W T (2007). Accuracy of ASTER level-2 thermal-infrared standard products of an agricultural area in Spain. *Remote Sensing of Environment* **106**(2): 146–153

Sobrino J A & Raissouni N (2000). Toward remote sensing methods for land cover dynamic monitoring. Application to Morocco. *International Journal of Remote Sensing* **21**: 353-366

Song C, Woodcock C E, Seto K C, Lenney M P & Macomber S A (2001). Classification and change detection using Landsat TM data: When and how to correct atmospheric effects? *Remote Sensing of Environment* **75**: 230-244

Xiao R, Ouyang Z, Zheng H, Li W, Schienke E W & Wang X (2007). Spatial pattern of impervious surfaces and their impacts on land surface temperature in Beijing, China. *Journal of Environmental Science (China)* **19**: 250-256

Valor E & Caselles V (1996). Mapping land surface emissivity from NDVI: Application to European, African and South American areas. *Remote Sensing of Environment* **57**: 167-184

Van de Griend A A & Owe M (1993). On the relationship between thermal emissivity and the normalized difference vegetation index for natural surfaces. *International Journal of Remote Sensing* **14**(6): 1119-1131

Zhang J, Wang Y & Li Y (2006). A C++ program for retrieving land surface temperature from the data of Landsat TM/ETM+ band 6. *Computers & Geosciences* **32**: 1796-1805